

# Localized ferromagnetic resonance force microscopy in permalloy-cobalt films

E. Nazaretski, I. Martin, K. C. Cha, E. A. Akhadov, and R. Movshovich

*Los Alamos National Laboratory, Los Alamos, NM 87545*

Yu. Obukhov, D. V. Pelekhov, and P. C. Hammel

*Department of Physics, Ohio State University, Columbus OH 43210,*

## Abstract

We report Ferromagnetic Resonance Force Microscopy (FMRFM) experiments on a justaposed continuous films of permalloy and cobalt. Our studies demonstrate the capability of FMRFM to perform local spectroscopy of different ferromagnetic materials. Theoretical analysis of the uniform resonance mode near the edge of the film agrees quantitatively with experimental data. Our experiments demonstrate the micron scale lateral resolution in determining local magnetic properties in continuous ferromagnetic samples.

PACS numbers: 07.79.Pk, 07.55.-w, 76.50.+g, 75.70.-i

Magnetic resonance force microscopy (MRFM) is attracting increasing attention as a result of its high spin sensitivity and excellent spatial resolution in paramagnetic and nuclear spin systems.[1, 2, 3, 4, 5, 6] MRFM studies on microfabricated and continuous ferromagnetic samples have been also performed. [7, 8, 9, 10, 11] Here we report FMRFM experiments performed on a non-overlapping permalloy (Py) and cobalt (Co) continuous films and demonstrate the capability of FMRFM to spectroscopically identify the distinct magnetic properties of two adjacent ferromagnetic films. We quantitatively model the resulting force signal strength and compare it with the experimental data.

The permalloy-cobalt sample is schematically shown in Fig. 1. A 20 nm thick Ti film was uniformly applied onto the surface of a 100  $\mu\text{m}$  thick Si (100) wafer. 20 nm of Co was deposited into a rectangular area ( $2.5 \times 5$  mm) defined in photoresist followed by the lift-off. A complimentary rectangular area of 20 nm thick Py was similarly defined and deposited. The entire structure was then coated with a 20 nm thick layer of Ti. The interface between the Co and Py regions was examined in a scanning electron microscope (SEM) and revealed a gap whose width varies between 3 and 6  $\mu\text{m}$  along the entire length of the sample (see SEM image in Fig. 1). An approximately  $1.7 \times 1.7$  mm<sup>2</sup> piece was cut and glued to the stripline resonator of the FMRFM apparatus and the film plane was oriented perpendicular to the direction of the external magnetic field  $H_{\text{ext}}$ . For FMRFM studies we used the cantilever with the spherical magnetic tip (see SEM image in Fig. 1) and its spatial field profile has been carefully characterized [12]. More details on the experimental apparatus can be found in Ref. [13]

In Fig. 2 we show the evolution of the FMRFM signal as a function of the lateral position and applied magnetic field. The cantilever was scanned across the interface between Co and Py, in the region indicated by arrows in Fig. 1. The FMRFM signal was recorded in two different regions of  $H_{\text{ext}}$  which correspond to Py and Co resonance fields for the microwave frequency of  $f_{RF}=9.35$  GHz. Insets in Fig. 2 show the evolution of the FMRFM spectra as a function of lateral position. The signal, reminiscent of those reported earlier in [14], is comprised of two distinctive contributions. The first, a negative signal which occurs at lower values of  $H_{\text{ext}}$  is a localized resonance originating from the region of the sample right under the cantilever tip where the probe field is strong and positive. The second contribution is positive and is observed at higher values of  $H_{\text{ext}}$ . This signal arises from a larger region of

sample remote from the tip which, therefore, experience a weak negative tip field; we will label this the “uniform resonance”. As seen in Fig. 2, at the beginning of the lateral scan the negative (lower field) resonance structure is present only in the Co spectrum (see inset a)). Near a lateral position of 9  $\mu\text{m}$  we see no localized signals (with negatively shifted  $H_{ext}$ ) for either the Py or the Co signals. However upon scanning further over the Py film, the Py resonance begins to show a localized signal, while the Co signal continues to show only a uniform (positively shifted  $H_{ext}$ ) signal (inset b)).

We analyze the uniform contribution to the FMRFM signals considering the case when the entire dynamic magnetization  $m$  is constant and the resonance field is only weakly affected by the probe. This approximation is valid for the large probe-sample distances (insets b) and c) in Fig. 2). The frequency of the uniform resonance in a thin film can be written as  $\omega_{RF}/\gamma = H_{ext} - 4\pi M_s$ , where  $4\pi M_s$  is the saturation magnetization and  $\gamma$  is the gyromagnetic ratio. FMRFM spectra shown in b) and c) insets in Fig. 2 yield the values of  $4\pi M_s = 8052$  G for Py and  $4\pi M_s = 15013$  G for Co respectively.

For quantitative analysis of the FMRFM data it is important to have an accurate estimate of the probe-sample separation. Magnetic Force Microscopy (MFM) measurements were used to calibrate the probe-sample separation. The cantilever was scanned across the Py - Co interface and changes in its resonance frequency were recorded. The gradient of the MFM force for a semi-infinite film can be written as follows:

$$\frac{\partial F}{\partial z} = 4m_p M_s L \frac{x(x^2 - 3z^2)}{(x^2 + z^2)^3}, \quad (1)$$

where  $m_p = 7 \times 10^{-9}$  emu is the probe magnetic moment [12] and  $L$  is the film thickness.  $z$  is the probe-film distance and  $x$  is the lateral position with respect to the film edge ( $x \geq 0$ ). MFM data were acquired at  $H_{ext} = 18255$  G, thus, both films were saturated. The MFM data and the fit to Eq. 1 are shown in Fig. 3a, yielding the tip-sample separation  $z \approx 4.4$   $\mu\text{m}$  and the films boundaries ( $x \leq 8$   $\mu\text{m}$  for Co and  $x \geq 11$   $\mu\text{m}$  for Py).

The tip field suppresses the uniform FMR mode in the region under the tip, and according to Obukhov *et al.* [15] the magnitude of the suppression depends on the tip-sample separation. It is described as partial suppression at distances  $z \gg \sqrt{\frac{2m_p}{\pi M_s L \alpha_0}}$  ( $\alpha_0$  is the first zero of the Bessel function  $J_0(\alpha_0) = 0$ ) and full suppression at  $z \ll \sqrt{\frac{2m_p}{\pi M_s L \alpha_0}}$ . The region of suppressed magnetization is confined to a region of radius  $r = \sqrt{2}z$ . FMRFM data discussed here were taken at the boundary of these two regions, thus we consider the regime of

full suppression, however we introduce the magnitude of the suppression as a fit parameter. Ferromagnetic resonance excitation generates a precessing transverse magnetization  $m$ , thus reducing  $M_z$ ; the change of  $M_z$  is  $\delta M_z = \sqrt{M_s^2 - m^2} - M_s \approx -m^2/2M_s$ . Here we modulate the amplitude of  $m$  with a 100% modulation depth at the cantilever resonance frequency. The FMRFM force exerted on a cantilever is  $F = -\int Lm^2/2M_s \cdot \partial H_p/\partial z dr'$ , where integration is performed over the entire film area. The total FMRFM force close the edge of the film is well approximated by

$$F = -\frac{m^2}{2M_s}L \left( \frac{4xz m_p}{(x^2 + z^2)^2} - \beta \int_S \theta(x') \frac{\partial H_p}{\partial z} (x - x') dr' \right), \quad (2)$$

where the first term describes the force between the probe and the semi-infinite film and the second term represents the force between the probe and the area of radius  $r = \sqrt{2}z$  under the tip. The Heaviside function  $\theta(x')$  represents the fact that the film is positioned at  $x' \geq 0$  and the dimensionless parameter  $\beta$  quantifies the degree of suppression of the uniform FMR mode. In Fig. 3b we plot the experimental data extracted from Fig. 2 and corresponding fits using Eq. 2. Fig. 3b demonstrates good qualitative and quantitative agreement between theory and experiment and demonstrates the validity of the model. It is important to mention that in our model we assume the dynamic magnetization  $m$  to be constant throughout the film. However,  $m$  may vary due to the change of the demagnetizing field e.g.  $-4\pi M_s$  far from the film boundary and  $-2\pi M_s$  at the film boundary. Our estimates show that  $m$  changes from a constant value in the film down to zero at the film edge. The length scale of this change is  $\pi M_s L/\Delta H \approx 1 \mu\text{m}$  ( $\Delta H$  is the linewidth of the uniform resonance), small compared to the probe-sample distance thus only weakly affecting the fits shown in Fig. 3b.

The spatial resolution of the uniform FMR mode shown in Fig. 3b is comparable to the MFM lateral resolution depicted in Fig. 3a and is determined by the probe-sample separation of  $z \approx 4.4 \mu\text{m}$ . However, it can be further improved by tracking the intensity of the FMRFM signal at values of  $H_{ext}$  lower than that of the uniform FMR mode (insets a) and d) in Fig. 2). In Fig. 3c we show the FMRFM force acquired at  $H_{ext} = 17960 \text{ G}$  for Co and  $H_{ext} = 11150 \text{ G}$  for Py respectively (values of  $H_{ext}$  are schematically indicated with dotted lines in Fig. 2). The contribution to the FMRFM signal at lower values of  $H_{ext}$  originates from the localized region of the sample under the probe. As seen in Fig. 3c the lateral resolution is on the order of  $3 \mu\text{m}$  (10% - 90% change in localized signal intensity)

and is determined by the FMR resonance linewidth and the spatial profile of the FMR mode under the tip. Further theoretical and numerical analysis is required to understand the evolution of the FMR modes excited under the probe in the presence of a strongly inhomogeneous tip field and boundaries of the sample.

In conclusion, we have obtained local FMR spectra in juxtaposed ferromagnetic samples and our quantitative model for the spatial variation of the uniform mode agrees well with experimental data. We have demonstrated spectroscopic imaging of Py and Co semi-infinite films with the spatial resolution for the tip induced resonance of  $\approx 3 \mu\text{m}$ .

The work performed at Los Alamos was supported by the US Department of Energy, and Center for Integrated Nanotechnologies at Los Alamos and Sandia National Laboratories. The work at OSU was supported by the US Department of Energy through grant DE-FG02-03ER46054.

- 
- [1] D. Rugar, C. S. Yannoni, and J. A. Sidles, *Nature* **360**, 563 (1993)
- [2] D. Rugar and O. Züger and S. Hoen and C. S. Yannoni and H. M. Vieth and R. D. Kendrick, *Science* **264**, 1560 (1994)
- [3] Z. Zhang, M. L. Roukes, and P. C. Hammel, *J. Appl. Phys.* **80**, 6931 (1996)
- [4] D. Rugar, R. Budakian, H. J. Mamin, and W. Chui, *Nature* **430**, 329 (2004)
- [5] C. L. Degen, Q. Lin, A. Hunkeler, U. Meier, M. Tomaselli, and B. H. Meier, *Phys. Rev. Lett.* **94**, 207601 (2005)
- [6] C. L. Degen, M. Poggio, H. J. Mamin, C. T. Rettner, and D. Rugar, *Proc. Natl. Acad. Sci.* **106**, 1313 (2009)
- [7] Z. Zhang, P. C. Hammel, and P. E. Wigen, *Appl. Phys. Lett.* **68**, 2005 (1996)
- [8] G. de Loubens, V.V. Naletov, O. Klein, J. Ben Youssef, F. Boust, and N. Vukadinovic, *Phys. Rev. Lett.* **98**, 127601 (2007)
- [9] Yu. Obukhov, D. V. Pelekhov, J. Kim, P. Banerjee, I. Martin, E. Nazaretski, R. Movshovich, S. An, T. J. Gramila, S. Batra, P. C. Hammel, *Phys. Rev. Lett.* **100**, 197601, (2008)
- [10] E. Nazaretski, D. V. Pelekhov, I. Martin, M. Zalalutdinov, D. Ponarin, A. Smirnov, P. C. Hammel, and R. Movshovich, *Phys. Rev. B* **79**, 132401 (2009)
- [11] E. Nazaretski, J. D. Thompson, M. Zalalutdinov, J. W. Baldwin, B. Houston, T. Mewes, D. V. Pelekhov, P. Wigen, P. C. Hammel, and R. Movshovich, *J. Appl. Phys.* **101**, 074905 (2007)
- [12] E. Nazaretski, E. A. Akhadov, I. Martin, D. V. Pelekhov, P. C. Hammel, and R. Movshovich, *Appl. Phys. Lett.* **92**, 214104 (2008).
- [13] E. Nazaretski, T. Mewes, D. Pelekhov, P. C. Hammel, and R. Movshovich, *AIP Conf. Proc.* **850**, 1641 (2006)
- [14] E. Nazaretski, D. V. Pelekhov, I. Martin, M. Zalalutdinov, J. W. Baldwin, T. Mewes, B. Houston, P. C. Hammel, and R. Movshovich, *Appl. Phys. Lett.* **90** 234105 (2007)
- [15] Yu. Obukhov, D. V. Pelekhov, E. Nazaretski, R. Movshovich, P. C. Hammel, *Appl. Phys. Lett.* **94**, 172508 (2008)

## Figure Caption

Figure 1: Schematic of the Co - Py sample. The arrows mark the scan range for spectra shown in Fig. 2. The SEM image on the right shows the gap between Py and Co. The SEM image on the left depicts the cantilever tip.

Figure 2: FMRFM force image as a function of  $H_{ext}$  and the lateral position. We show the Co and Py forces in the upper and lower panels respectively. Insets a) - d) demonstrate the evolution of the FMRFM signal as a function of lateral position indicated on the left-hand side of each inset. Vertical dashed lines show the boundaries of the Co and Py films. The horizontal dashed-dotted lines are drawn through the values of  $H_{ext} = 18255$  G for Co and  $H_{ext} = 11296$  G for Py respectively and correspond to the uniform resonance (see Fig. 3b). The horizontal dotted lines at  $H_{ext} = 17960$  G and  $H_{ext} = 11150$  G for Co and Py respectively, mark the localized FMRFM signals. Experimental parameters:  $T = 11$  K,  $f_{RF} = 9.35$  GHz, probe-sample distance  $\approx 5.6$   $\mu\text{m}$ .

Figure 3: a) MFM data acquired at  $H_{ext} = 18255$  G, solid line is the fit to Eq. 1. b) FMRFM force data for the uniform ferromagnetic resonance (FMR) modes.  $H_{ext} = 18255$  G for Co (squares) and  $H_{ext} = 11296$  G for Py (circles). Solid and dashed lines are fits of Eq. 2 to the data. Fit parameters:  $m/M_s = 0.0014$ ,  $\beta = 0.65$  for Co and  $m/M_s = 0.0028$ ,  $\beta = 0.5$  for Py. c) FMRFM force for the localized (close to the probe) FMR mode acquired at  $H_{ext} = 17960$  G for Co (squares) and  $H_{ext} = 11150$  G for Py (circles). The lateral resolution is better than  $3$   $\mu\text{m}$ .

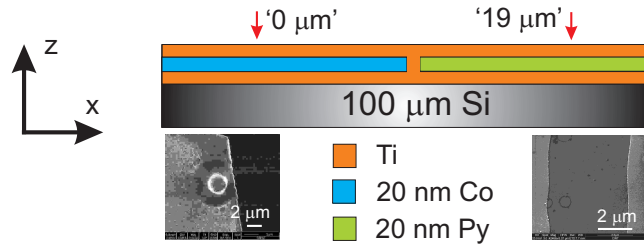


FIG. 1:

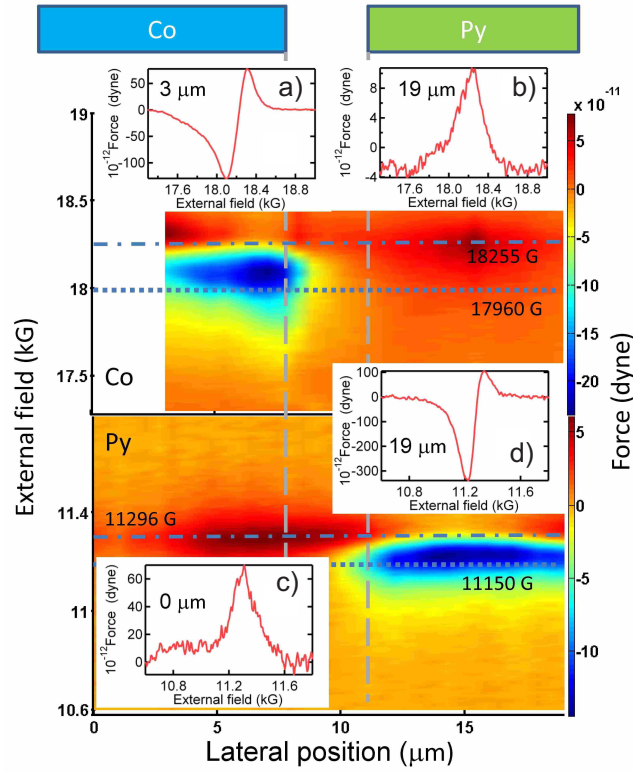


FIG. 2:



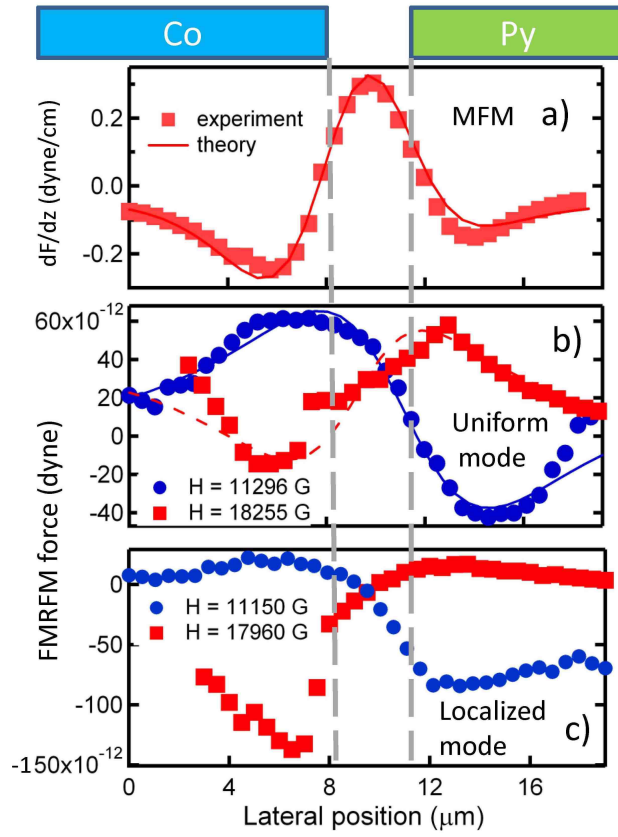


FIG. 3: